Tune-out wavelengths for the $2\,^3S_1$ state of the Li^+ ion

Fang-Fei Wu,* Ke Deng, and Ze-Huang Lu

MOE Key Laboratory of Fundamental Physical Quantities Measurement, Hubei Key Laboratory of Gravitation and Quantum Physics, PGMF and School of Physics, Huazhong University of Science and Technology, Wuhan 430074, People's Republic of China

(Received 20 July 2022; accepted 6 October 2022; published 25 October 2022)

Configuration interaction calculations are performed to determine the dipole polarizabilities and tune-out wavelengths for the $2\,^3S_1$ state in Li^+ ion. The finite nuclear mass correction is given by including the mass shift operator in the Dirac-Coulomb-Breit Hamiltonian directly, while the QED correction to dynamic dipole polarizabilities is evaluated by using the perturbation theory. The tune-out wavelengths for the $2\,^3S_1$ ($M_J = 0$) and $2\,^3S_1$ ($M_J = \pm 1$) states are 159.620 55(6) nm and 159.631 14(6) nm, respectively. And the QED correction for 159 nm tune-out wavelength is 43 ppm. In addition, we obtain the static dipole polarizability for the $2\,^3S_1$ ($M_J = \pm 1$) state to be 46.857 03(4) a.u., in which the contribution from QED is 70 ppm. The 159 nm tune-out wavelength and the static dipole polarizability of $2\,^3S_1$ state might provide a test of atomic structure theory.

DOI: 10.1103/PhysRevA.106.042816

I. INTRODUCTION

High-precision theoretical calculations and spectroscopic measurements of transition frequencies for light atoms and molecules are actively studied as a way of testing quantum electrodynamics (QED) theory in the last decade [1–7]. For helium, the relative precision of frequency measurements for some transitions has reached the 10^{-12} level [3,4]. This experimental precision is sufficient to determine the nuclear charge radii of ^{3}He and ^{4}He. However, the nuclear charge radii extracted from $2\,^3S \to 2\,^3P$ and $2\,^3S_1 \to 2\,^1S_0$ transitions have a 4σ discrepancy [1,3,8–11]. Even combined with the theoretical investigations [12,13], the discrepancy still exists. Recently, Patkóš *et al.* have performed the calculations of the complete $m\alpha^7$-order QED effects for the $2\,^3S$ and $2\,^3P$ states [6], but the discrepancy between theory and experiment for the $2\,^3S \to 3\,^3D$ and $2\,^3P \to 3\,^3D$ transitions has not been solved.

In 2013, Mitroy and Tang proposed that the 413 nm tune-out wavelength for the metastable state of helium would provide a nonenergy test of atomic structure theory [14]. Henceforth, Henson *et al.* performed the first measurement for this tune-out wavelength [15] in 2015. And the tune-out wavelength including the relativistic, finite nuclear mass, and QED effects was calculated by Zhang *et al.* using the relativistic configuration interaction method [16]. These results are consistent at the ppm level. In recent research, the accuracy of experimental result for 413 nm tune-out wavelength has reached 0.4 ppm, which differs from theory by 1.7 times the measurement uncertainty [17]. Compared with helium, the leading order QED effect of Li^+ is about five times larger, since the leading order QED correction increases in proportion to the Z^4 (Z is the nuclear charge number). Therefore, Li^+ ion is also a suitable system to test the atomic structure theory.

For the Li^+ ion, the theoretical energies that account for all relativistic and QED effects up to $m\alpha^6$ order of the low-lying states are given in Ref. [18]. And there are many theoretical results of the dipole polarizability for the low-lying states based on different methods [19–32]. However, only a few works have investigated the dynamic polarizabilities of the $2\,^3S$ state [21,22,32]. The rigorous upper and lower bounds to the dynamic polarizabilities of the $2\,^3S$ state are given by Glover and Weinhold [21,22]. Zhang *et al.* obtained the dynamic dipole polarizabilities and tune-out wavelengths for the four lowest triplet states, and magic wavelengths for the $2\,^3S \to 3\,^3S$, $2\,^3S \to 2\,^3P$, and $2\,^3S \to 3\,^3P$ transitions by using the nonrelativistic configuration interaction method [32]. To our knowledge, the relativistic, finite nuclear mass, and QED effects of dynamic dipole polarizabilities for the $2\,^3S$ state have rarely been investigated.

Recently, the Zemach radii of $^6Li^+$ and $^7Li^+$ ions have been extracted by comparing high-precision calculations and measurements [33]. The difference of Zemach radii for the $^6Li^+$ ion between the value in Ref. [33] and nuclear physics value [34] reveals the anomalous nuclear structure for the $^6Li^+$ ion. The measurements of hyperfine and fine-structure splittings for the $2\,^3S_1$ and $2\,^3P_J$ states have now attained an uncertainty less than 100 kHz [35]. The results of the $2\,^3P_J$ state are one order of magnitude more accurate than those of previous measurements [36]. These precise calculations and measurements make it possible to explore the nuclear structure and test the atomic structure theory.

In addition, the technology of the optical frequency comb in the extreme ultraviolet (XUV) region has been developed in the past two decades [37–39]. With the advent of the XUV frequency comb, the measurement of the $1S \to 2S$ two-photon transition in He^+, He, and Li^+ has been achieved [40–43]. The development of experimental technology will prompt

*fangfeiwu@hust.edu.cn

new research into testing the atomic structure theory of the Li^+ ion.

In this paper, the relativistic configuration interaction (RCI) calculations including finite nuclear mass correction are performed for the dynamic dipole polarizabilities for the $2\,^3S_1$ state of the Li^+ ion. QED correction of dynamic dipole polarizability is evaluated by the perturbation method using nonrelativistic energies and wave functions. The accuracy of static dipole polarizability has achieved 0.4 ppm. We also determine the tune-out wavelengths for the $2\,^3S_1$ ($M_J = 0$) and $2\,^3S_1$ ($M_J = \pm 1$) states to be 159.620 55(6) nm and 159.631 14(6) nm, respectively. The finite nuclear mass and QED corrections of the 159 nm tune-out wavelength are 261 ppm and 43 ppm, respectively. The 159 nm tune-out wavelength is sensitive to finite nuclear mass, relativistic, and QED effects, which would provide an independent nonenergy testing for the atomic structure theory of Li^+ ion. Atomic units (a.u.) are used throughout this paper unless otherwise specified.

II. THEORETICAL METHOD

The present calculations are based on the Dirac-Coulomb-Breit (DCB) Hamiltonian, which includes the mass shift (MS) operator $H_{\rm MS}$ directly,

$$H = \sum_{i=1}^{2}\left[c\boldsymbol{\alpha}_i\cdot\boldsymbol{p}_i + \beta m_e c^2 - \frac{Z}{r_i}\right] + \frac{1}{r_{12}} - \frac{1}{2r_{12}}[\boldsymbol{\alpha}_1\cdot\boldsymbol{\alpha}_2 + (\boldsymbol{\alpha}_1\cdot\hat{\boldsymbol{r}}_{12})(\boldsymbol{\alpha}_2\cdot\hat{\boldsymbol{r}}_{12})] + H_{\rm MS}, \quad (1)$$

where $c = 137.035999074$ is the speed of light [44], $\boldsymbol{\alpha}_i$ and β are the Dirac matrices, $\boldsymbol{p}_i$ is the momentum operator for the ith electron, m_e is the electron mass, Z is the nuclear charge, $\hat{\boldsymbol{r}}_{12}$ is the unit vector of the electron-electron distance $\boldsymbol{r}_{12}$, and the first term in the second row of Eq. (1) is the Breit operator with the retardation effect excluded. The MS operator $H_{\rm MS}$ includes the normal ($H_{\rm NMS}$) and specific mass shift ($H_{\rm SMS}$) operators [45],

$$H_{\rm MS} = H_{\rm NMS} + H_{\rm SMS}, \quad (2)$$

$$H_{\rm NMS} = \frac{1}{2M}\sum_i\left[\boldsymbol{p}_i^2 - \frac{\alpha Z}{r_i}\left(\boldsymbol{\alpha}_i + \frac{(\boldsymbol{\alpha}_i\cdot\boldsymbol{r}_i)\boldsymbol{r}_i}{r_i^2}\right)\cdot\boldsymbol{p}_i\right], \quad (3)$$

$$H_{\rm SMS} = \frac{1}{2M}\sum_{i\neq j}\left[\boldsymbol{p}_i\cdot\boldsymbol{p}_j - \frac{\alpha Z}{r_i}\left(\boldsymbol{\alpha}_i + \frac{(\boldsymbol{\alpha}_i\cdot\boldsymbol{r}_i)\boldsymbol{r}_i}{r_i^2}\right)\cdot\boldsymbol{p}_j\right], \quad (4)$$

where M is the nuclear mass, and α is the fine-structure constant. The Notre Dame basis sets [46] of N number of B-spline functions are used to construct the single-electron wave functions. And the wave function for a state of Li^+ with angular momentum (J, M_J) is expanded as a linear combination of the configuration-state wave functions, which are constructed by the single-electron wave functions. The negative-energy B-spline orbitals of single-electron are excluded in present RCI calculations.

The dynamic dipole polarizability for the magnetic sublevel $|\gamma_g J_g M_{J_g}\rangle$ in the linearly polarized light is

$$\alpha_1(\omega) = \alpha_1^S(\omega) + \frac{3M_{J_g}^2 - J_g(J_g+1)}{J_g(2J_g-1)}\alpha_1^T(\omega), \quad (5)$$

where $\alpha_1^S(\omega)$ and $\alpha_1^T(\omega)$ are, respectively, the scalar and tensor dipole polarizabilities, which can be expressed as the summation over all intermediate states $|\gamma_n J_n M_{J_n}\rangle$, including the nonrelativistic forbidden transition and the continuum,

$$\alpha_1^S(\omega) = \sum_{n\neq g}\frac{f_{gn}^{(1)}}{(\Delta E_{gn})^2 - \omega^2}, \quad (6)$$

$$\alpha_1^T(\omega) = \sum_{n\neq g}(-1)^{J_g+J_n}\sqrt{\frac{30(2J_g+1)J_g(2J_g-1)}{(2J_g+3)(J_g+1)}} \times\begin{Bmatrix}1 & 1 & 2\\ J_g & J_g & J_n\end{Bmatrix}\frac{f_{gn}^{(1)}}{(\Delta E_{gn})^2-\omega^2}. \quad (7)$$

In the above equations, the dipole oscillator strength $f_{gn}^{(1)}$ is defined as

$$f_{gn}^{(1)} = \frac{2|\langle N_g J_g\|T\|N_n J_n\rangle|^2\Delta E_{gn}}{3(2J_g+1)}, \quad (8)$$

where $\Delta E_{gn} = E_n - E_g$ is the transition energy from the initial state $|\gamma_g J_g\rangle$ to the intermediate state $|\gamma_n J_n\rangle$, ω is the photon energy of the external field, and T is the dipole transition operator.

QED corrections to dynamic polarizability and tune-out wavelength are evaluated by the perturbation theory using nonrelativistic energies and wave functions, which are obtained by nonrelativistic configuration interaction (NRCI) calculations [47,48]. The QED correction of the dynamic polarizability [16] for $|g\rangle$ state is

$$\delta\alpha_1^{\rm QED}(\omega) = 2\left[\sum_n\frac{\langle g|D|n\rangle\langle n|D|g\rangle\langle g|\delta H_{\rm QED}|g\rangle[(E_n-E_g)^2+\omega^2]}{[(E_n-E_g)^2-\omega^2]^2} - 2\sum_{nm}\frac{\langle g|D|n\rangle\langle n|D|m\rangle\langle m|\delta H_{\rm QED}|g\rangle(E_n-E_g)}{[(E_n-E_g)^2-\omega^2](E_m-E_g)} - \sum_{nm}\frac{\langle g|D|n\rangle\langle n|\delta H_{\rm QED}|m\rangle\langle m|D|g\rangle[(E_n-E_g)(E_m-E_g)+\omega^2]}{[(E_n-E_g)^2-\omega^2][(E_m-E_g)^2-\omega^2]}\right], \quad (9)$$

where $|n\rangle$ and $|m\rangle$ are the intermediate states, and $\delta H_{\rm QED}$ is the QED operator, expanded to $m\alpha^5$ and $m\alpha^6$order [18],

$$H_{\rm QED}^{(3)} = \frac{4Z\alpha^3}{3}\left\{\frac{19}{30} + \ln[(Z\alpha)^{-2}] - \ln\left(\frac{k_0}{Z^2}\right)\right\}[\delta^3(r_1)+\delta^3(r_2)] + O(r_{12}), \quad (10)$$

$$H_{\rm QED}^{(4)} = \alpha^4\left\{\left[-\frac{9\zeta(3)}{4\pi^2} - \frac{2179}{648\pi^2} + \frac{3\ln(2)}{2} - \frac{10}{27}\right]\pi Z + \left[\frac{427}{96} - 2\ln(2)\right]\pi Z^2\right\}[\delta^3(r_1)+\delta^3(r_2)]. \quad (11)$$

TABLE I. Convergence test of energy (in a.u.) for the 2 $^3S_1$ state of Li^+ ion. The numbers in parentheses are computational uncertainties.

(N, ℓ_{max})	NRCI	RCI	RCI($^7Li^+$)
(40,7)	−5.110 727 210	−5.111 343 477	−5.110 942 441
(40,8)	−5.110 727 267	−5.111 343 542	−5.110 942 480
(40,9)	−5.110 727 296	−5.111 343 559	−5.110 942 533
(40,10)	−5.110 727 311	−5.111 343 576	−5.110 942 545
(45,10)	−5.110 727 330	−5.111 343 611	−5.110 942 544
(50,10)	−5.110 727 338	−5.111 343 595	−5.110 942 555
Extrap.	−5.110 727 36(4)	−5.111 343 63(4)	−5.110 942 55(4)
Ref. [18]	−5.110 727 373	−5.111 343 494	−5.110 942 448

Here $\ln k_0 = 5.17107628(2)$ is the Bethe logarithm for the 2 $^3S_1$ state of Li^+ ion [49], $\zeta(x)$ is the Riemann Zeta function, and $O(r_{12})$ represents the remaining term connected with r_{12} of $m\alpha^5$ order.

III. ENERGIES AND OSCILLATOR STRENGTHS

In the present calculations, we used the N B-spline functions of order $k = 7$ with the maximum partial wave ℓ_{max} in a cavity with radius of 150, which accommodates the initial state and the corresponding intermediate states for calculating the dynamic dipole polarizabilities for the 2 $^3S_1$ state.

Table I gives the convergence test of energy for the 2 $^3S_1$ state of Li^+ ion. The NRCI and RCI columns represent nonrelativistic and relativistic energies without finite nuclear mass effect, respectively. The last column represents the energy of $^7Li^+$ ion including relativistic and finite nuclear mass corrections. The extrapolation was done by assuming that the ratio between two successive differences in energies stays constant as the maximum number of partial wave ℓ_{max} and the number of B-spline functions N become infinitely large. The nonrelativistic result −5.110 727 36(4) without finite nuclear mass correction agrees well with the value −5.110 727 373 in Ref. [18]. The relativistic results in the last two columns have seven same digits compared with the perturbation results [18], which includes the $m\alpha^4$-order relativistic correction and leading order finite nuclear mass correction. From the NRCI and RCI columns, the relativistic correction to the energy of the 2 $^3S_1$ state is −0.000 616 27(6). Comparing the extrapolated values between RCI and RCI($^7Li^+$) columns, it is found that the finite nuclear mass effect for the $^7Li^+(2^3S_1)$ state is 0.000 401 08(6).

For 2 ^3P_J states, the present NRCI energy is −5.027 715 62(4), which has eight same digits with the result of −5.027 715 681 [18]. The RCI energies of 2 ^3P_J states, seen from Table II, are in good agreement with the perturbation results in Ref. [18]. Comparing the NRCI and RCI energies, the relativistic corrections of the 2 $^3P_0$, 2 $^3P_1$, and 2 $^3P_2$ states are −0.000 522 61(6), −0.000 546 24(6), and −0.000 536 72(6), respectively. And the finite nuclear mass effect 0.000 369 31(6) for $^7Li^+$ ion is obtained by comparing the values in Table II.

In present RCI calculations, the single-electron wave functions are obtained by solving the single-electron Dirac equation. The Breit operator and the mass shift operator H_{MS} are added in the Hamiltonian directly. Therefore, the relativistic correction of single-electron and all corrections from the Breit operator and the mass shift operator H_{MS} are included in the RCI results; i.e., the present RCI results include the $m\alpha^4$- and higher-order single-electron relativistic corrections, the $m\alpha^4$-order and a part of the $m\alpha^6$-order relativistic corrections of the electron-electron interaction, and the nonrelativistic and leading order relativistic finite nuclear mass corrections. However, the perturbation results from Ref. [18] only can extract the $m\alpha^4$-order relativistic corrections and the nonrelativistic and leading order relativistic finite nuclear mass corrections, since the sum of the $m\alpha^6$-order relativistic and QED corrections are given in Ref. [18], and none of them can not be extracted separately. Therefore, the main difference between the present RCI results and the values of the perturbation method is a part of the $m\alpha^6$-order relativistic corrections.

TABLE II. Comparison of energies (in a.u.) for the 2 ^3P_J states of Li^+ ion. The numbers in parentheses are computational uncertainties.

	RCI	RCI($^7Li^+$)
2 $^3P_0$	−5.028 238 23(4)	−5.027 868 92(4)
	−5.028 238 151 [18]	−5.027 868 829 [18]
2 $^3P_1$	−5.028 261 86(4)	−5.027 892 55(4)
	−5.028 261 761 [18]	−5.027 892 438 [18]
2 $^3P_2$	−5.028 252 34(4)	−5.027 883 03(4)
	−5.028 252 310 [18]	−5.027 882 990 [18]

The oscillator strengths for the 2 $^3S_1 \rightarrow n\,^3P_J$ ($n = 2, 3$) transitions of Li^+ ion are shown in Table III. The NRCI and RCI results have six or seven significant digits. The nonrelativistic results for the listed transitions in Table III are consistent with the explicitly correlated wave function calculations of Ref. [50]. For the 2 $^3S \rightarrow 2\,^3P$ transition, the present nonrelativistic result of 0.307 940 4(1) is more accurate than the value of 0.307 944 [50] by one order of magnitude, and has six same digits with the value of 0.307 940 2 in Ref. [51]. By comparing the RCI and RCI($^7Li^+$) columns in Table III, the finite nuclear mass correction of the oscillator strengths for 2 $^3S_1 \rightarrow 2, 3\,^3P_J$ transitions is at the 10^{-5} level.

IV. STATIC POLARIZABILITIES AND TUNE-OUT WAVELENGTHS

With the energies and oscillator strengths obtained, the dipole polarizabilities can be calculated by using the

TABLE III. Comparison of oscillator strengths for 2 $^3S_1 \rightarrow n\,^3P_J$ ($n = 2, 3$) transitions of Li^+ ion. The numbers in parentheses are computational uncertainties.

$n\,^3P_J$	NRCI	RCI	RCI($^7Li^+$)
2 $^3P_0$		0.034 250 63(1)	0.034 240 81(1)
2 $^3P_1$	0.307 940 4(1)	0.102 717 35(4)	0.102 687 87(4)
2 $^3P_2$		0.171 221 26(6)	0.171 171 20(6)
3 $^3P_0$		0.020 762 22(1)	0.020 770 73(1)
3 $^3P_1$	0.187 054 2(1)	0.062 305 22(2)	0.062 330 73(2)
3 $^3P_2$		0.103 829 50(8)	0.103 872 06(8)

TABLE IV. Convergence test of static dipole polarizability $\alpha_1(0)$ and tune-out wavelength λ_t (in nm) for the $2\,^3S_1$ state of Li^+ ion. The numbers in parentheses are computational uncertainties.

	RCI		RCI($^7Li^+$)	
(N, ℓ_{max})	$\alpha_1(0)$ $(M_J = 0/\pm 1)$	λ_t $(M_J = 0/\pm 1)$	$\alpha_1(0)$ $(M_J = 0/\pm 1)$	λ_t $(M_J = 0/\pm 1)$
(40,7)	46.826 935/46.831 204	159.571 709/159.582 300	46.849 371/46.853 645	159.613 337/159.623 940
(40,8)	46.826 970/46.831 239	159.571 817/159.582 411	46.849 428/46.853 702	159.613 490/159.624 092
(40,9)	46.826 993/46.831 263	159.571 879/159.582 475	46.849 422/46.853 698	159.613 494/159.624 103
(40,10)	46.827 010/46.831 278	159.571 924/159.582 516	46.849 440/46.853 715	159.613 545/159.624 149
(45,10)	46.826 993/46.831 262	159.571 896/159.582 489	46.849 460/46.853 732	159.613 583/159.624 181
(50,10)	46.826 997/46.831 268	159.571 906/159.582 505	46.849 453/46.853 726	159.613 571/159.624 172
Extrap.	46.826 98(4)/46.831 25(4)	159.571 88(6)/159.582 48(6)	46.849 47(4)/46.853 74(4)	159.613 61(6)/159.624 20(6)

sum-over-states method. Then, the tune-out wavelengths are extracted by making the dynamic dipole polarizabilities equal to zero. In the nonrelativistic calculations, the static dipole polarizability of $2\,^3S$ state is 46.879 80(1), which agrees well with the Hylleraas result of 46.879 802 3(7) [30]. Table IV presents the convergence test of the static dipole polarizability $\alpha_1(0)$ and the tune-out wavelength λ_t for the $2\,^3S_1$ state in RCI calculations. The relativistic static dipole polarizabilities are 46.826 98(4) and 46.831 25(4) for the $M_J = 0$ and $M_J = \pm 1$ sublevels, respectively. The averaged values of relativistic static dipole polarizabilities over the magnetic sublevels for $^\infty Li^+$ and $^7Li^+$ are 46.830 18(4) and 46.852 67(4), respectively.

The 159 nm tune-out wavelength for the $2\,^3S_1$ state is located at the edge of the $2\,^3S \to 3\,^3P$ resonance transitions; it is seen clearly from Fig. 1. The NRCI result of tune-out wavelength for the $2\,^3S_1$ state is 159.671 74(2) nm. From Table IV, the RCI tune-out wavelengths are convergence to seven digits. The tune-out wavelengths for the $2\,^3S_1$ ($M_J = 0$) and $2\,^3S_1$ ($M_J = \pm 1$) states of $^\infty Li^+$ are 159.571 88(6) and 159.582 48(6) nm, respectively. Comparing the results of 159 nm tune-out wavelength between RCI and RCI($^7Li^+$) columns, it is found that the finite nuclear mass effect increases the 159 nm tune-out wavelength by 0.0417 3(8) nm. The averaged value of RCI tune-out wavelengths over the magnetic sublevels $^\infty Li^+$ and $^7Li^+$ are 159.579 83(6) nm and 159.621 55(6) nm, respectively.

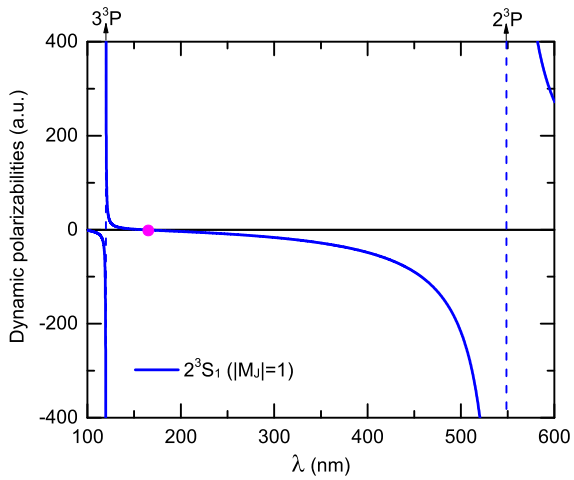

FIG. 1. Dynamic dipole polarizabilities of Li^+ ion for the wavelength 100 nm $\leqslant \lambda \leqslant$ 600 nm. The solid blue line represents the dynamic dipole polarizabilities for $2\,^3S_1$ ($M_J = \pm 1$) state. The tune-out wavelength marked as a solid magenta circle, and the blue dash lines denote the resonance transitions.

In addition, the QED corrections to the static dipole polarizabilities and the tune-out wavelengths for $2\,^3S$ state are also evaluated. The $m\alpha^5$-order QED correction to energy of $2\,^3S_1$ state given by Yerokhin and Pachucki is 0.000 075 206 [18]. In our calculations, the $m\alpha^5$-order QED correction omitting the $O(r_{12})$ term of Eq. (11) is 0.000 075 234. This indicates that the contribution from the $O(r_{12})$ term is -2.8×10^{-8}. And the $m\alpha^6$-order QED correction is 2.25×10^{-6}, which is two orders of magnitude larger than the contribution from the $O(r_{12})$ term. So in this work, the QED corrections to the static dipole polarizabilities and tune-out wavelengths are calculated by omitting the $O(r_{12})$ contribution. Furthermore, the recoil effect contribution to the $m\alpha^5$-order QED correction of static dipole polarizability and tune-out wavelength is at the 10^{-6} level for $^7Li^+$, which is smaller by one order of magnitude than the uncertainty of RCI result. Therefore, the recoil effect contribution to the $m\alpha^5$-order QED correction can be neglected at the present calculation accuracy.

The convergence test for the $m\alpha^5$- and $m\alpha^6$-order QED corrections to the static dipole polarizability and the 159 nm tune-out wavelength of the $2\,^3S_1$ state is given in Table V. The extrapolated values of QED correction for static dipole polarizability and tune-out wavelength have five converged digits. The $\delta\alpha_1^{\rm QED}(0)(m\alpha^5)$ and $\delta\alpha_1^{\rm QED}(0)(m\alpha^6)$ are 0.003 188 89(2) and 0.000 095 535(1), respectively. The $m\alpha^5$-order QED correction contributes 6.734 40(2) pm to 159 nm tune-out wavelength, which is 33 times larger than the $m\alpha^6$-order QED correction.

Moreover, the finite nuclear size correction of the static dipole polarizability and the tune-out wavelength of $2\,^3S_1$ state are also evaluated by adopting the operator of $4\pi r^2_{^7Li^+}[\delta^3(r_1) + \delta^3(r_2)]/3$ for a uniform charge distribution. The nuclear charge radius $r_{^7Li^+}$ of $^7Li^+$ ion is 2.444(42) fm [52]. The finite nuclear size correction increases the static dipole polarizability and the tune-out wavelength by 3.5×10^{-6} and 7.3 fm, respectively. Under the current calculation accuracy, this correction can be ignored. In particular, the correction from the electric-field dependence term $\partial^2_\varepsilon \ln k_0$ of the Bethe logarithm is not evaluated in the present calculations.

The contributions to the static dipole polarizability $\alpha_1(0)$ and the 159 nm tune-out wavelength λ_t for the $2\,^3S_1$ state of

TABLE V. Convergence test of QED correction of static dipole polarizability $\alpha_1(0)$ and tune-out λ_t (in nm) for the 2 ^3S state of Li^+ ion. $\delta\alpha_1^{QED}(0)(m\alpha^5)$ and $\delta\alpha_1^{QED}(0)(m\alpha^6)$ represent the $m\alpha^5$- and $m\alpha^6$-order QED corrections to $\alpha_1(0)$, respectively. The numbers in parentheses are computational uncertainties.

(N, ℓ_{max})	$\delta\alpha_1^{QED}(0)(m\alpha^5)$	$\delta\alpha_1^{QED}(0)(m\alpha^6)$	$\delta\lambda_t^{QED}(m\alpha^5)$	$\delta\lambda_t^{QED}(m\alpha^6)$
(40,7)	0.003 188 869 516	0.000 095 534 388	0.006 734 360 956	0.000 201 747 252
(40,8)	0.003 188 878 459	0.000 095 534 656	0.006 734 381 680	0.000 201 747 873
(40,9)	0.003 188 882 681	0.000 095 534 783	0.006 734 391 565	0.000 201 748 168
(40,10)	0.003 188 884 839	0.000 095 534 848	0.006 734 396 653	0.000 201 748 321
Extrap.	0.003 188 89(2)	0.000 095 535(1)	0.006 734 40(2)	0.000 201 749(1)

Li^+ ion can be seen clearly from Table VI and Fig. 2. The sum of finite nuclear mass and QED corrections of 0.025 77(4) is added to the RCI static dipole polarizability; we obtained the $\alpha_1(0)$ of 2 $^3S_1$ ($M_J = \pm1$) state as 46.857 03(4). Taking the finite nuclear mass and QED corrections into account, the tune-out wavelengths for 2 $^3S_1$ ($M_J = 0$) and 2 $^3S_1$ ($M_J = \pm1$) states are 159.620 55(6) and 159.631 14(6) nm, respectively. The QED correction for the tune-out wavelength of the 2 $^3S_1$ state is 43 ppm. If the measurements for this tune-out wavelength achieve an accuracy of 0.001 nm, the influence of QED effects would to be identified. Therefore, the 159 nm tune-out wavelength for the Li^+(2 $^3S_1$) state might provide the nonenergy test for the atomic structure theory.

V. CONCLUSION

We have calculated the dynamic dipole polarizabilities of the 2 $^3S_1$ state for Li^+ ion based on the DCB Hamiltonian with the finite nuclear mass effect included directly. The QED corrections on the dynamic dipole polarizabilities are estimated by using perturbation theory. The tune-out wavelengths for the 2 $^3S_1$ ($M_J = 0$) and 2 $^3S_1$ ($M_J = \pm1$) states are 159.620 55(6) nm and 159.631 14(6) nm, respectively. The finite nuclear mass correction of 159 nm tune-out wavelength for the 2 $^3S_1$ state is 0.041 73(8) nm, and the QED correction is 43 ppm. This tune-out wavelength may be used to test the atomic structure theory in the future. In addition, the static dipole polarizabilities for the $M_J = 0$ and $M_J = \pm1$ sublevels of the 2 $^3S_1$ state are 46.852 76(4) and 46.857 03(4), respectively. The hyperfine structure correction of static dipole polarizability and tune-out wavelength for the 2 $^3S_1$ state will be calculated in the future.

TABLE VI. Contributions to the static dipole polarizability $\alpha_1(0)$ and the 159 nm tune-out wavelength λ_t (in nm) for the 2 $^3S_1$ ($M_J = 0, \pm1$) state of Li^+ ion. FNM and FNS represent the finite nuclear mass and finite nuclear size corrections, respectively. The numbers in parentheses are computational uncertainties.

Contrib.	M_J	$\alpha_1(0)$	λ_t
RCI	0	46.826 98(4)	159.571 88(6)
	±1	46.831 25(4)	159.582 48(6)
RCI+FNM	0	46.849 47(4)	159.613 61(6)
	±1	46.853 74(4)	159.624 20(6)
$m\alpha^5$ QED		0.003 188 89(2)	0.006 734 40(2)
$m\alpha^6$ QED		0.000 095 535(1)	0.000 201 749(1)
FNS		0.000 003 5	0.000 007 3
Total	0	46.852 76(4)	159.620 55(6)
	±1	46.857 03(4)	159.631 14(6)

ACKNOWLEDGMENTS

F.-F.W. thanks Li-Yan Tang, Yong-Hui Zhang, Yong-Bo Tang, and Ting-Yun Shi for their help on the study of the configuration interaction method. This work was supported by the National Natural Science Foundation of China under Grant No. 12004124. The authors acknowledge the Beijing Super Cloud Computing Center (BSCC) for providing HPC resources that have contributed to the research results reported within this paper.

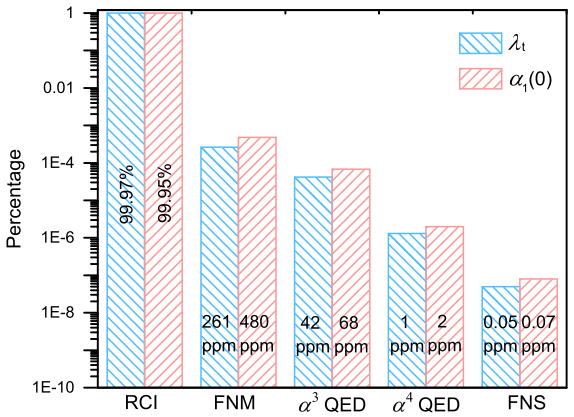

FIG. 2. The relative contributions of finite nuclear mass (FNM), QED, finite nuclear size (FNS) and corrections to the static polarizability $\alpha_1(0)$ and tune-out wavelength λ_t for 2 $^3S_1$ ($M_J = \pm1$) state of $^7Li^+$ ion.

[1] R. van Rooij, J. S. Borbely, J. Simonet, M. D. Hoogerland, K. S. E. Eikema, R. A. Rozendaal, and W. Vassen, Science **333**, 196 (2011).

[2] K. Pachucki, V. Patkóš, and V. A. Yerokhin, Phys. Rev. A **95**, 062510 (2017).

[3] X. Zheng, Y. R. Sun, J.-J. Chen, W. Jiang, K. Pachucki, and S.-M. Hu, Phys. Rev. Lett. **119**, 263002 (2017).

[4] R. J. Rengelink, Y. van der Werf, R. P. M. J. W. Notermans, R. Jannin, K. S. E. Eikema, M. D. Hoogerland, and W. Vassen, Nat. Phys. **14**, 1132 (2018).

[5] Y.-J. Huang, Y.-C. Guan, Y.-C. Huang, T.-H. Suen, J.-L. Peng, L.-B. Wang, and J.-T. Shy, Phys. Rev. A **97**, 032516 (2018).

[6] V. Patkóš, V. A. Yerokhin, and K. Pachucki, Phys. Rev. A **103**, 042809 (2021).

[7] G. Clausen, P. Jansen, S. Scheidegger, J. A. Agner, H. Schmutz, and F. Merkt, Phys. Rev. Lett. **127**, 093001 (2021).

[8] D. Shiner, R. Dixson, and V. Vedantham, Phys. Rev. Lett. **74**, 3553 (1995).

[9] P. C. Pastor, G. Giusfredi, P. De Natale, G. Hagel, C. de Mauro, and M. Inguscio, Phys. Rev. Lett. **92**, 023001 (2004).

[10] D. C. Morton, Q. Wu, and G. W. F. Drake, Phys. Rev. A **73**, 034502 (2006).

[11] P. Cancio Pastor, L. Consolino, G. Giusfredi, P. De Natale, M. Inguscio, V. A. Yerokhin, and K. Pachucki, Phys. Rev. Lett. **108**, 143001 (2012).

[12] K. Pachucki and V. A. Yerokhin, J. Phys. Chem. Ref. Data **44**, 031206 (2015).

[13] V. Patkóš, V. A. Yerokhin, and K. Pachucki, Phys. Rev. A **94**, 052508 (2016).

[14] J. Mitroy and L.-Y. Tang, Phys. Rev. A **88**, 052515 (2013).

[15] B. M. Henson, R. I. Khakimov, R. G. Dall, K. G. H. Baldwin, L.-Y. Tang, and A. G. Truscott, Phys. Rev. Lett. **115**, 043004 (2015).

[16] Y.-H. Zhang, F.-F. Wu, P.-P. Zhang, L.-Y. Tang, J.-Y. Zhang, K. G. H. Baldwin, and T.-Y. Shi, Phys. Rev. A **99**, 040502(R) (2019).

[17] B. M. Henson, J. A. Ross, K. F. Thomas, C. N. Kuhn, D. K. Shin, S. S. Hodgman, Y.-H. Zhang, L.-Y. Tang, G. W. F. Drake, A. T. Bondy, A. G. Truscott, and K. G. H. Baldwin, Science **376**, 199 (2022).

[18] V. A. Yerokhin and K. Pachucki, Phys. Rev. A **81**, 022507 (2010).

[19] K. T. Chung, Phys. Rev. A **4**, 7 (1971).

[20] R. M. Glover and F. Weinhold, J. Chem. Phys. **65**, 4913 (1976).

[21] R. M. Glover and F. Weinhold, J. Chem. Phys. **66**, 185 (1977).

[22] R. M. Glover and F. Weinhold, J. Chem. Phys. **66**, 191 (1977).

[23] D. M. Bishop and M. Rérat, J. Chem. Phys. **91**, 5489 (1989).

[24] M.-K. Chen, J. Phys. B: At., Mol. Opt. Phys. **28**, 1349 (1995).

[25] W. R. Johnson and K. T. Cheng, Phys. Rev. A **53**, 1375 (1996).

[26] A. K. Bhatia and R. J. Drachman, Phys. Rev. A **55**, 1842 (1997).

[27] A. K. Bhatia and R. J. Drachman, Can. J. Phys. **75**, 11 (1997).

[28] J.-M. Zhu, B.-L. Zhou, and Z.-C. Yan, Chem. Phys. Lett. **313**, 184 (1999).

[29] Z.-C. Yan, J.-M. Zhu, and B.-L. Zhou, Phys. Rev. A **62**, 034501 (2000).

[30] J.-M. Zhu, B.-L. Zhou, and Z.-C. Yan, Mol. Phys. **98**, 529 (2000).

[31] I. S. Lim, J. K. Laerdahl, and P. Schwerdtfeger, J. Chem. Phys. **116**, 172 (2002).

[32] Y.-H. Zhang, L.-Y. Tang, X.-Z. Zhang, and T.-Y. Shi, Chin. Phys. B **25**, 103101 (2016).

[33] X.-Q. Qi, P.-P. Zhang, Z.-C. Yan, G. W. F. Drake, Z.-X. Zhong, T.-Y. Shi, S.-L. Chen, Y. Huang, H. Guan, and K.-L. Gao, Phys. Rev. Lett. **125**, 183002 (2020).

[34] V. A. Yerokhin, Phys. Rev. A **78**, 012513 (2008).

[35] H. Guan, S. Chen, X.-Q. Qi, S. Liang, W. Sun, P. Zhou, Y. Huang, P.-P. Zhang, Z.-X. Zhong, Z.-C. Yan, G. W. F. Drake, T.-Y. Shi, and K. Gao, Phys. Rev. A **102**, 030801(R) (2020).

[36] J. J. Clarke and W. A. van Wijngaarden, Phys. Rev. A **67**, 012506 (2003).

[37] R. J. Jones, K. D. Moll, M. J. Thorpe, and J. Ye, Phys. Rev. Lett. **94**, 193201 (2005).

[38] A. Cingöz, D. C. Yost, T. K. Allison, A. Ruehl, M. E. Fermann, I. Hartl, and J. Ye, Nature (London) **482**, 68 (2012).

[39] J. Zhang, L.-Q. Hua, Z. Chen, M.-F. Zhu, C. Gong, and X.-J. Liu, Chin. Phys. Lett. **37**, 124203 (2020).

[40] S. D. Bergeson, A. Balakrishnan, K. G. H. Baldwin, T. B. Lucatorto, J. P. Marangos, T. J. McIlrath, T. R. O'Brian, S. L. Rolston, C. J. Sansonetti, J. Wen, N. Westbrook, C. H. Cheng, and E. E. Eyler, Phys. Rev. Lett. **80**, 3475 (1998).

[41] M. Haas, U. D. Jentschura, C. H. Keitel, N. Kolachevsky, M. Herrmann, P. Fendel, M. Fischer, T. Udem, R. Holzwarth, T. W. Hänsch, M. O. Scully, and G. S. Agarwal, Phys. Rev. A **73**, 052501 (2006).

[42] E. E. Eyler, D. E. Chieda, M. C. Stowe, M. J. Thorpe, T. R. Schibli, and J. Ye, Eur. Phys. J. D **48**, 43 (2008).

[43] M. Herrmann, M. Haas, U. D. Jentschura, F. Kottmann, D. Leibfried, G. Saathoff, C. Gohle, A. Ozawa, V. Batteiger, S. Knünz, N. Kolachevsky, H. A. Schüssler, T. W. Hänsch, and T. Udem, Phys. Rev. A **79**, 052505 (2009).

[44] P. J. Mohr, B. N. Taylor, and D. B. Newell, Rev. Mod. Phys. **84**, 1527 (2012).

[45] I. I. Tupitsyn, V. M. Shabaev, J. R. Crespo López-Urrutia, I. Draganić, R. S. Orts, and J. Ullrich, Phys. Rev. A **68**, 022511 (2003).

[46] W. R. Johnson, S. A. Blundell, and J. Sapirstein, Phys. Rev. A **37**, 307 (1988).

[47] Y.-H. Zhang, L.-Y. Tang, X.-Z. Zhang, and T.-Y. Shi, Phys. Rev. A **92**, 012515 (2015).

[48] Y.-H. Zhang, L.-Y. Tang, X.-Z. Zhang, and T.-Y. Shi, Phys. Rev. A **93**, 052516 (2016).

[49] G. W. F. Drake and S. P. Goldman, Can. J. Phys. **77**, 835 (1999).

[50] N. M. Cann and A. J. Thakkar, Phys. Rev. A **46**, 5397 (1992).

[51] B. Schiff, C. L. Pekeris, and Y. Accad, Phys. Rev. A **4**, 885 (1971).

[52] W. Nörtershäuser, T. Neff, R. Sánchez, and I. Sick, Phys. Rev. C **84**, 024307 (2011).